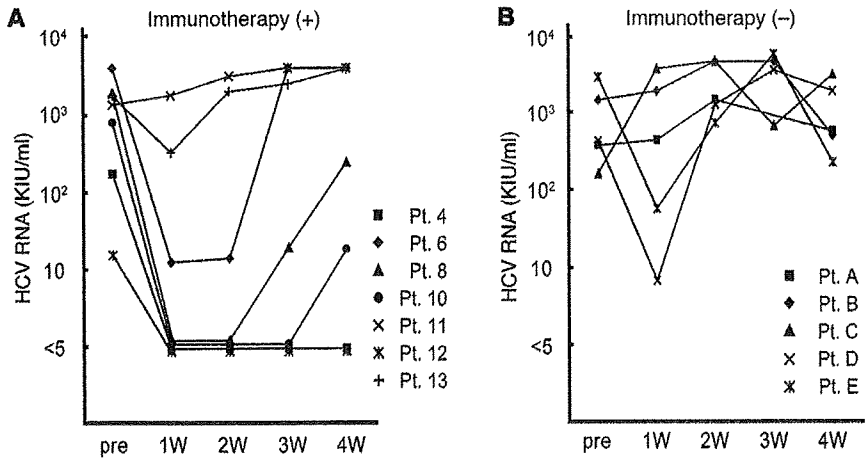

Figure 3
Serial measurement of the HCV RNA titers of LT recipients after LT. The HCV RNA titers in the sera of LT recipients who received immunotherapy were markedly lower than those in the sera of LT recipients who did not receive the therapy during the first month after LT. Each line with a different symbol represents serial HCV RNA titers from an LT recipient who received (+) (**A**; $n = 7$) and 1 who did not receive (–) (**B**; $n = 5$) the immunotherapy after LT. KIU, kilo international unit; pre, pre LT; W, week.

tion that NK cell–conditioned media have an enhanced expression of signal transducer and activator of transcription 1, a nuclear factor that is essential in IFN-γ–mediated antiviral pathways. It has also been reported that hepatocytes cultured in NK cell–conditioned media express higher levels of IFN-α/β, IFN regulatory factor 3, and IFN regulatory factor 7, confirming that NK cells play a key role in suppressing HCV infection of and replication in human hepatocytes in an IFN-dependent manner (23). Similar to recent reports, in the present study, we demonstrated that the NK cells among the IL-2/OKT3–treated liver lymphocytes released soluble factors, predominantly IFN-γ, thus suppressing HCV replication (Figures 5–7).

In addition to NK cells, NKT cells are thought to be involved in eliciting innate responses against infection; however, the role of NKT cells in controlling HCV infection/replication remains unclear. One report has indicated that the number of NKT cells in patients with chronic HCV infection does not differ from that in healthy donors; however, activated NKT cells in HCV-infected patients produce higher levels of IL-13 – but comparable levels of IFN-γ – than those in healthy subjects, showing that NKT cells are biased toward T-helper 2-type responses in chronic HCV infection (24). Another recent report has shown that the sustained response of patients with chronic hepatitis C to treatment with IFN-α and ribavirin is closely associated with increased dynamism of NK and NKT cells in the liver, implicating an NKT cell–mediated mechanism in anti-HCV activity (25). Here, we have described that NKT as well as NK cells in the IL-2/

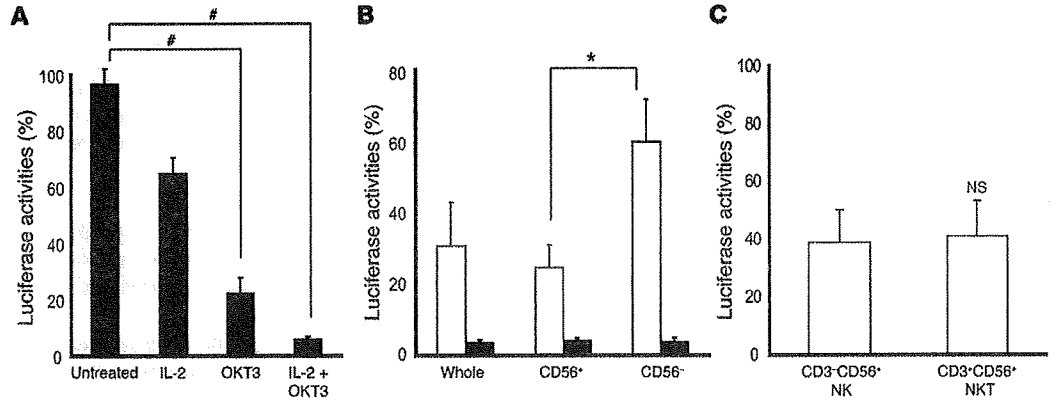

Figure 4
The cultivation of liver lymphocytes with IL-2/OKT3 markedly promoted anti-HCV activity. (**A**) Activation by IL-2 and OKT3 significantly promoted the anti-HCV effect of the liver allograft–derived lymphocytes that were cultured in complete medium with and without IL-2 (100 JRU/ml) for 3 days. OKT3 (1 μg/ml) was then added 1 day before coculturing with HCV replicon cells, at the indicated time. The bar graphs indicate the luciferase activities of the cells in each group. Data are presented as mean ± SEM ($n = 5$). Statistical analyses were performed using the Mann-Whitney *U* test with Bonferroni correction after the Kruskal-Wallis *H* test. $^{\#}P < 0.01$ for OKT3 and IL-2/OKT3 treatment versus no treatment. (**B**) $CD56^+$ fraction, including NK and NKT cells, strongly inhibited HCV replication. The culture conditions are described in **A**. By magnetic cell sorting, $CD56^+$ and $CD56^-$ fractions were isolated from the activated lymphocytes and analyzed for anti-HCV activity. The bar graphs indicate the luciferase activities of the cells in each group (IL-2–treated group, white bars; IL-2 plus OKT3–treated group, black bars). Whole, whole lymphocytes. Data are presented as mean ± SEM ($n = 5$). Statistical analyses were performed using the Mann-Whitney *U* test. $^*P < 0.05$ for $CD56^+$ fraction versus $CD56^-$ fraction. (**C**) Anti-HCV effect of NK cells was almost identical to that of NKT cells after IL-2 activation. The liver allograft–derived lymphocytes were cultured in complete medium with IL-2 (100 JRU/ml) for 3 days. By magnetic sorting, $CD3^-CD56^+$ (NK) and $CD3^+CD56^+$ (NKT) fractions were isolated from the activated lymphocytes and analyzed for anti-HCV activity. Data are presented as mean ± SEM ($n = 6$).

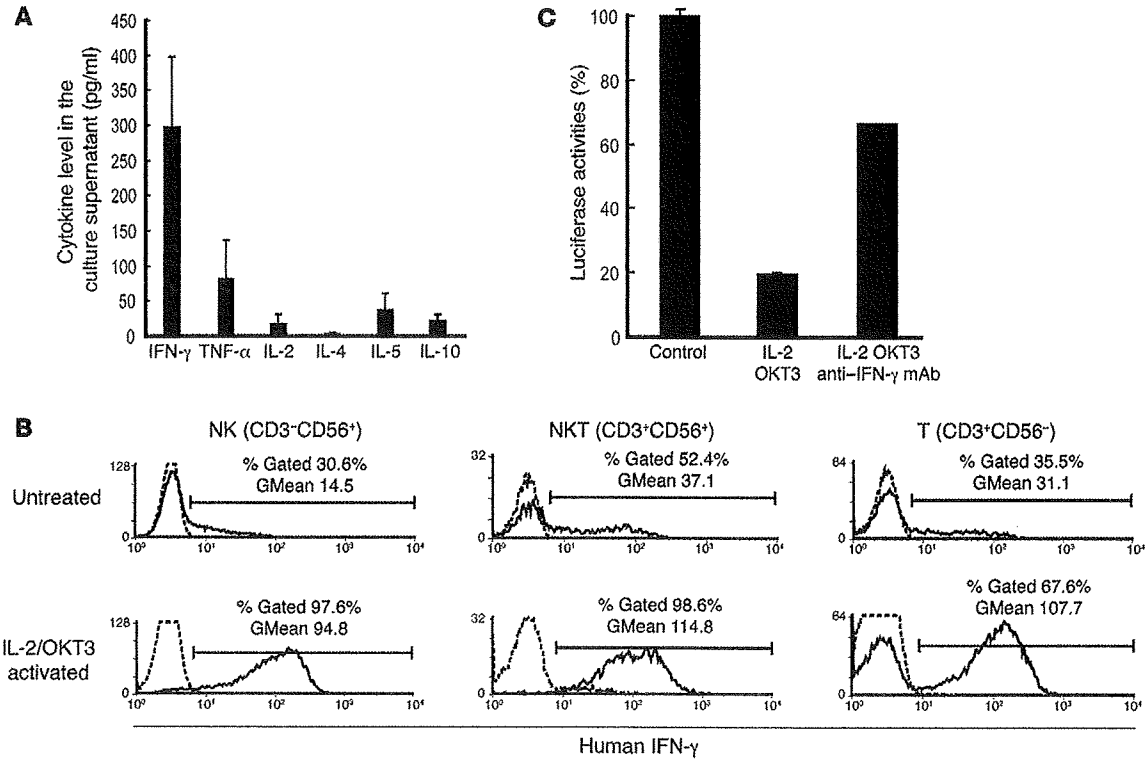

Figure 5

Anti-HCV activity of IL-2/OKT3–treated liver lymphocytes was dependent on their IFN-γ secretion ability. (**A**) IFN-γ was the major cytokine released from the cultured cells. The bar graphs indicate the concentrations of various cytokines (IFN-γ, TNF-α, IL-2, IL-4, IL-5, and IL-10) detected in the coculture supernatant by CBA. Data are presented as mean ± SEM (n = 3). (**B**) The effects of IL-2 and OKT3 (100 JRU/ml and 1 μg/ml, respectively) on IFN-γ production by stimulated $CD3^-CD56^+$ NK, $CD3^+CD56^+$ NKT, and $CD3^+CD56^-$ T cells were evaluated by a combination of cell surface and cytoplasmic mAb staining and subsequent flow cytometric analysis. Histograms represent the log fluorescence intensities obtained upon staining for IFN-γ after gating of each fraction. Dotted lines represent negative control staining with isotype-matched mAbs. Horizontal lines indicate the gated portion of lymphocytes. GMean, geometric mean fluorescent intensity. (**C**) Blocking of IFN-γ with mAb (100 μg/ml) elucidated the marked role played by IFN-γ in producing the anti-HCV effect. The bar graphs indicate the luciferase activities of the cells in each group. Data are presented as mean ± SEM of a representative triplicate sample.

OKT3-treated liver lymphocytes could play a vital role in controlling HCV replication in hepatic cells via an IFN-γ–associated mechanism (Figures 5 and 6).

Therefore, in the early phase of HCV reinfection after LT, the effects of IFN-γ secretion from adoptively injected liver lymphocytes may include inhibition of HCV virion production, which is probably caused by suppression of viral RNA and protein synthesis without immune lysis of intact hepatic cells. This IFN-γ secretion from both $CD3^+CD56^+$ NKT cells and $CD3^+$ T cells was markedly upregulated after treatment with OKT3, which was originally used to prevent GVHD (Figure 5B). This is possibly because of the potent mitogenic activity of OKT3 that induces the activation of $CD3^+CD56^+$ NKT cells and $CD3^+$ T cells. However, the administration of OKT3-coated cells in vivo results in the opsonization and subsequent trapping and/or lympholysis of cells by the reticuloendothelial system (26–28). Thus, GVHD is prevented in LT recipients treated with adoptive immunotherapy.

Our finding that the IL-2/OKT3–treated liver lymphocytes controlled HCV replication via an IFN-γ–associated mechanism can lead to the clinical application of recombinant IFN-γ for anti-HCV treatment. However, a clinically applicable dose of recombinant IFN-γ could not induce significant inhibitory effects on HCV viremia in the previous study (29). Based on the accumulation of adoptively injected IL-2/OKT3–treated liver lymphocytes in the liver of human hepatocyte-chimeric mice (data not shown), the immunotherapy with the liver lymphocytes would provide sufficient IFN-γ to the HCV-infected site.

It has been recently reported that HCV-specific $CD8^+$ T cells exert strong antiviral effects by both cytopathic and IFN-γ–mediated noncytopathic effector functions (30). However, in patients with chronic HCV infection, dysfunction and functional restoration of HCV-specific $CD8^+$ T cell responses have been reported (31). Since HCV-specific $CD8^+$ T cell defects may be important in persistent HCV infections, correcting these defects is considered to our knowledge to be a novel approach to treat HCV infection. Further studies are required to investigate whether activation of NK or NKT cells functionally restores HCV-specific $CD8^+$ T cells.

In conclusion, adoptive immunotherapy using IL-2/OKT3–treated liver lymphocytes containing abundant NK and NKT cells could mount remarkable anti-HCV responses in HCV-infected LT recipients, although its effects were incomplete or transient. Treatment-related improvements, such as defining the best schedule and frequency of cell inoculation and developing more potent effectors, could improve clinical benefits.

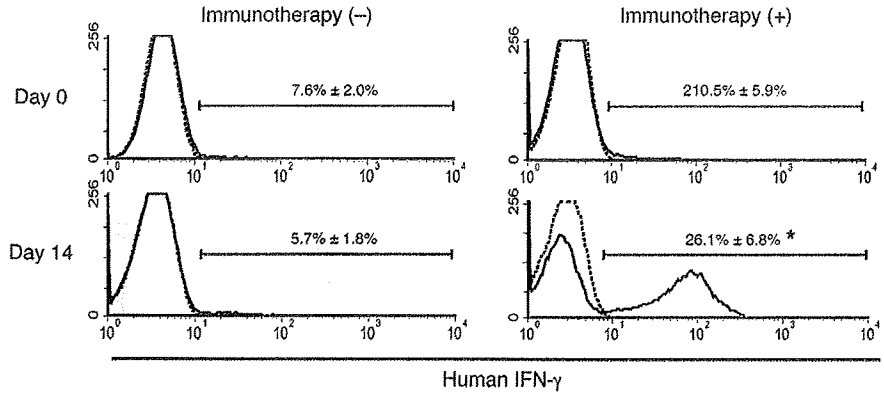

Figure 6
Adoptive immunotherapy with IL-2/OKT3–treated liver lymphocytes induced the production of IFN-γ in the LT recipients. At 14 days after LT, the number of IFN-γ–secreting cells in the peripheral blood of LT recipients treated with the adoptive immunotherapy (+) with IL-2/OKT3–treated liver lymphocytes, including NK and NKT cells, was significantly higher than that in the peripheral blood of untreated LT recipients (–). Histograms represent the proportion (percentage) of IFN-γ–positive cells among the mononuclear cells obtained from the peripheral blood of the immunotherapy ($n = 4$) and control group ($n = 4$) LT recipients. Dotted lines represent negative control staining with isotype-matched mAbs. Horizontal lines indicate the gated portion of lymphocytes. Data are presented as mean ± SEM. Histogram profiles shown are representative of 4 independent experiments. Statistical analyses were performed using the Mann-Whitney *U* test. $^*P < 0.05$ for immunotherapy group versus control group.

Methods

Subjects. All the human liver samples were collected at Hiroshima University Hospital. Tissue specimens were collected after approval from the Institutional Review Board of Hiroshima University and after written informed consent was obtained from the patients. The use of immunotherapy with IL-2/OKT3–treated liver lymphocytes was approved by the Clinical Institutional Ethical Review Board of Hiroshima University. Written informed consent was obtained from all of the patients. This approach was successfully used in 14 cirrhotic patients with HCC undergoing clinical LT (Tables 1 and 2). Of these 14 patients, 7 had chronic HCV infection. Five other LT recipients with chronic HCV infection did not agree to receive this immunotherapy during the trial period. HCV RNA was qualitatively detected in the sera of these patients by a standardized qualitative RT-PCR assay (Amplicor HCV monitor, version 2.0; Roche Diagnostics) every week during the first month after LT.

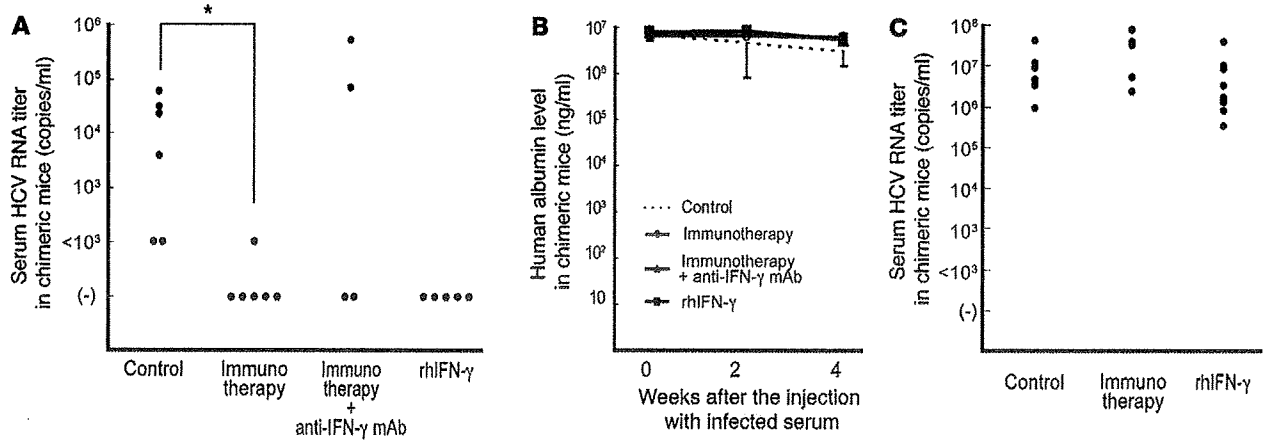

Figure 7
Adoptive immunotherapy with IL-2/OKT3–treated liver lymphocytes prevented HCV infection in human hepatocyte–chimeric mice. (**A**) Human hepatocyte–chimeric mice were intravenously injected with human serum samples positive for HCV genotype 1b. Two weeks after injecting the infected serum, the mice were intraperitoneally inoculated with IL-2/OKT3–treated liver lymphocytes (20×10^6 cells/mouse; $n = 6$) for adoptive immunotherapy. When indicated, anti-human IFN-γ mAb was injected intraperitoneally 1 day before the immunotherapy ($n = 4$). Intraperitoneal injection of recombinant human IFN-γ (rhIFN-γ) was commenced at 2 weeks after injecting the infected serum ($n = 5$). The untreated mice served as controls ($n = 6$). The dot plots represent serum HCV RNA titers in each chimeric mouse 4 weeks after the injecting the infected serum. Statistical analyses were performed using the Mann-Whitney *U* test. $^*P < 0.01$ for immunotherapy group versus control group. (**B**) The lines represent serial changes in human serum albumin levels in the sera of the mice indicated above. Data are presented as mean ± SEM. (**C**) IL-2/OKT3–treated liver lymphocytes (20×10^6 cells/mouse) were intraperitoneally inoculated 4 weeks after the injection with the infected serum ($n = 5$) for adoptive immunotherapy. Intraperitoneal injection of recombinant human IFN-γ was commenced 4 weeks after the injecting the infected serum ($n = 9$). The untreated mice served as controls ($n = 9$). The dot plots represent serum HCV RNA titers in each chimeric mouse 6 weeks after injection with the infected serum.

Isolation of lymphocytes from liver allograft perfusate. Donor hepatectomy and the transplantation procedure were performed as described previously (32). After hepatectomy, ex vivo perfusion of the liver allograft was performed through the portal vein. Liver allograft–derived lymphocytes were isolated by gradient centrifugation with Ficoll-Paque (GE Healthcare Bio-Sciences AB).

Adoptive transfer of IL-2/OKT3–treated liver lymphocytes. Liver lymphocytes were cultured with human recombinant IL-2 (100 Japanese reference units/ml [JRU/ml]; Takeda) in complete medium at 37°C in a 5% CO_2 incubator for 3 days. One day before the infusion, 1 μg/ml of OKT3 (Janssen-Kyowa) was added in order to opsonize the $CD3^+$ fraction. On the day of infusion, the cells were washed twice with 0.9% sodium chloride and resuspended with 5% human serum albumin in 0.9% sodium chloride for injection (Figure 1). The viability of the cells was assessed by the dye-exclusion test, and the cells were checked twice for possible contamination by bacteria, fungi, and endotoxins.

Cytotoxicity assay. A ^{51}Cr-release assay was done as previously described (5), using HepG2 tumor cells (Japanese Cancer Research Resources Bank) as targets. Briefly, ^{51}Cr-labeled target tumor cells were added for 4 hours at 37°C to effector cells in round-bottomed 96-well microtiter plates (BD Biosciences — Discovery Labware). The percentage of specific ^{51}Cr release was calculated as follows: % cytotoxicity = [(cpm of experimental release − cpm of spontaneous release)/(cpm of maximum release − cpm of spontaneous release)] × 100. All the assays were performed in triplicate.

Flow cytometry. Flow cytometric analyses were performed using a FACSCalibur dual-laser cytometer (BD Biosciences). The following mAbs were used for the surface staining of the lymphocytes: FITC-conjugated anti-CD3 mAb (clone HIT3a; BD Biosciences — Pharmingen); PE-conjugated anti-CD56 mAb (clone B159; BD Biosciences — Pharmingen); and biotinylated anti-TRAIL (biotin-conjugated anti-TRAIL) mAb (clone RIK-2; eBioscience). The biotinylated mAb was visualized using APC-streptavidin (BD Biosciences — Pharmingen). Dead cells identified by light scatter and propidium iodide staining were excluded from the analysis. IFN-γ production in the lymphocytes was measured by a combination of cell surface and cytoplasmic mAb staining and subsequent flow cytometric analysis, as described previously (33).

Isolation of $CD56^+$ and $CD56^-$ fractions and that of NK and NKT cells. Liver allograft–derived lymphocytes were separated into a $CD56^+$ fraction — including NK and NKT cells — and a $CD56^-$ fraction by using auto MACS (Miltenyi Biotec) with anti-human CD56 microbeads (Miltenyi Biotec) according to the manufacturer's instructions. The NK and NKT cells were also isolated by magnetic cell sorting, using the human NK cell isolation kit or human $CD3^+CD56^+$ NKT cell isolation kit (Miltenyi Biotec). The purity of the isolated fractions was assessed by flow cytometric analysis, and only the fractions with purities greater than 90% were used for functional studies.

Coculture with HCV replicon–containing hepatic cells. An HCV subgenomic replicon plasmid, pRep-Feo, was derived from pRep-Neo (originally, pHCVIbneo-delS; ref. 34). The pRep-Feo carries a fusion gene comprising firefly luciferase (*Fluc*) and neomycin phosphotransferase, as described elsewhere (35, 36). After culture in the presence of G418 (Invitrogen), pRep-Feo cell lines stably expressing the replicons were established. For coculture experiments, transwell tissue culture plates (pore size, 1 μm; Costar) were used. HCV replicon-containing hepatic cells (10^5 cells) were incubated in the lower compartment with different numbers of lymphocytes in the upper compartment. The hepatic cells in the lower compartments were collected 48 hours after coculture for the luciferase assay. Luciferase activities were measured with a luminometer (Lumat LB9501; Promega), using the Bright-Glo Luciferase Assay System (Promega).

Cytometric bead array. Cytokine (IFN-γ, TNF-α, IL-2, IL-4, IL-5, IL-10) levels in the coculture assay supernatants were measured with the FACSCalibur dual-laser cytometer (BD Biosciences), using a BD Human Th1/Th2 Cytokine Cytometric Bead Array (CBA) Kit according to the manufacturer's instructions.

Generation of human hepatocyte–chimeric mice. Generation of the $uPA^{+/+}$ $SCID^{+/+}$ mice and transplantation of human hepatocytes were performed as described recently by our group (20, 37). Mouse serum concentrations of human serum albumin correlated with the repopulation index (20), and these were measured as described previously (37).

In vivo studies using human hepatocyte–chimeric mice. Human hepatocyte-chimeric mice were intravenously injected with 50 μl of the human serum samples positive for HCV genotype 1b. The serum HCV RNA titer in human hepatocyte-chimeric mice was detected by nested PCR, as previously described (38, 39). All animal protocols described in this study were performed in accordance with the guidelines and with approval of the Ethics Review Committee of Animal Experimentation of the Graduate School of Biomedical Sciences, Hiroshima University. Either 2 or 4 weeks after injecting the infected serum, the mice were intraperitoneally inoculated with IL-2/OKT3–treated liver lymphocytes (20×10^6 cells/mouse) for adoptive immunotherapy. When indicated, anti-human IFN-γ mAb (R&D Systems) (1.5 mg/mouse) was injected intraperitoneally 1 day before the immunotherapy. In a separate experiment, intraperitoneal injection of recombinant human IFN-γ (Imunomax-γ; Shionogi & Co. Ltd.) was commenced at either 2 or 4 weeks after injecting the infected serum. IFN-γ was administered as follows: 1×10^5 IU on the first day and thereafter 2×10^4 IU/day for 13 days.

Statistics. Data are presented as mean ± SEM. The statistical differences of the results were analyzed by 2-tailed, paired Student's *t* test, Mann-Whitney *U* test, and Mann-Whitney *U* test with Bonferroni correction after the Kruskal-Wallis *H* test, using the Stat View program. *P* values of 0.05 or less were considered statistically significant.

Acknowledgments

This work was supported in part by a Grant-in-Aid for Exploratory Research (19659323) from the Japan Society for the Promotion of Science. We thank Kentaro Ide, Toshimitsu Irei, Hiroyuki Tahara, Masataka Banshodani, Nabin Basnet, Hirofumi Tazawa, and Keiko Kajitani for their advice and encouragement and Yuko Ishida for expert technical assistance.

Received for publication December 17, 2008, and accepted in revised form July 29, 2009.

Address correspondence to: Hideki Ohdan, Department of Surgery, Division of Frontier Medical Science, Programs for Biomedical Research, Graduate School of Biomedical Sciences, Hiroshima University, 1-2-3 Kasumi, Minami-ku, Hiroshima 734-8551, Japan. Phone: 81-82-257-5220; Fax: 81-82-257-5224; E-mail: hohdan@hiroshima-u.ac.jp. Or to: Kazuaki Chayama, Department of Medicine and Molecular Science, Division of Frontier Medical Science, Programs for Biomedical Research, Graduate School of Biomedical Sciences, Hiroshima University, 1-2-3 Kasumi, Minami-ku, Hiroshima 734-8551, Japan. Phone: 81-82-257-5190; Fax: 81-82-257-5194; E-mail: chayama@hiroshima-u.ac.jp.

1. Petrovic, L.M. 2006. Early recurrence of hepatitis C virus infection after liver transplantation. *Liver Transpl.* **12**:S32–S37.
2. Brown, R.S. 2005. Hepatitis C and liver transplantation. *Nature.* **436**:973–978.
3. Garcia-Retortillo, M., et al. 2002. Hepatitis C virus kinetics during and immediately after liver transplantation. *Hepatology.* **35**:680–687.
4. Berenguer, M. 2002. Natural history of recurrent hepatitis C. *Liver Transpl.* **8**:S14–S18.
5. Ishiyama, K., et al. 2006. Difference in cytotoxicity against hepatocellular carcinoma between liver and periphery natural killer cells in humans. *Hepatology.* **43**:362–372.
6. Ohira, M., et al. 2006. Adoptive transfer of TRAIL-

expressing natural killer cells prevents recurrence of hepatocellular carcinoma after partial hepatectomy. *Transplantation.* **82**:1712–1719.
7. Miller, J.S., et al. 2005. Successful adoptive transfer and in vivo expansion of human haploidentical NK cells in patients with cancer. *Blood.* **105**:3051–3057.
8. Hirata, M., et al. 1998. Increase in natural killer cell activity following living-related liver transplantation. *Transpl. Int.* **11**(Suppl. 1):S185–S188.
9. Harada, N., et al. 2004. IL-12 gene therapy is an effective therapeutic strategy for hepatocellular carcinoma in immunosuppressed mice. *J. Immunol.* **173**:6635–6644.
10. Golden-Mason, L., and Rosen, H.R. 2006. Natural killer cells: primary target for hepatitis C virus immune evasion strategies? *Liver Transpl.* **12**:363–372.
11. Li, Y., et al. 2004. Natural killer cells inhibit hepatitis C virus expression. *J. Leukoc. Biol.* **76**:1171–1179.
12. Deignan, T., et al. 2002. Decrease in hepatic CD56(+) T cells and V alpha 24(+) natural killer T cells in chronic hepatitis C viral infection. *J. Hepatol.* **37**:101–108.
13. Durante-Mangoni, E., et al. 2004. Hepatic CD1d expression in hepatitis C virus infection and recognition by resident proinflammatory CD1d-reactive T cells. *J. Immunol.* **173**:2159–2166.
14. Kawarabayashi, N., et al. 2000. Decrease of CD56(+)T cells and natural killer cells in cirrhotic livers with hepatitis C may be involved in their susceptibility to hepatocellular carcinoma. *Hepatology.* **32**:962–969.
15. Rosen, H.R., et al. 2008. Pretransplantation CD56(+) innate lymphocyte populations associated with severity of hepatitis C virus recurrence. *Liver Transpl.* **14**:31–40.
16. Doherty, D.G., et al. 1999. The human liver contains multiple populations of NK cells, T cells, and CD3+CD56+ natural T cells with distinct cytotoxic activities and Th1, Th2, and Th0 cytokine secretion patterns. *J. Immunol.* **163**:2314–2321.
17. Mazzaferro, V., et al. 1996. Liver transplantation for the treatment of small hepatocellular carcinomas in patients with cirrhosis. *N. Engl. J. Med.* **334**:693–699.
18. Mercer, D.F., et al. 2001. Hepatitis C virus replication in mice with chimeric human livers. *Nat. Med.* **7**:927–933.
19. Kneteman, N.M., et al. 2006. Anti-HCV therapies in chimeric scid-Alb/uPA mice parallel outcomes in human clinical application. *Hepatology.* **43**:1346–1353.
20. Tateno, C., et al. 2004. Near completely humanized liver in mice shows human-type metabolic responses to drugs. *Am. J. Pathol.* **165**:901–912.
21. Tseng, C.T., and Klimpel, G.R. 2002. Binding of the hepatitis C virus envelope protein E2 to CD81 inhibits natural killer cell functions. *J. Exp. Med.* **195**:43–49.
22. Crotta, S., et al. 2002. Inhibition of natural killer cells through engagement of CD81 by the major hepatitis C virus envelope protein. *J. Exp. Med.* **195**:35–41.
23. Wang, S.H., et al. 2008. Natural killer cells suppress full cycle HCV infection of human hepatocytes. *J. Viral Hepat.* **15**:855–864.
24. Kanto, T., and Hayashi, N. 2007. Innate immunity in hepatitis C virus infection: Interplay among dendritic cells, natural killer cells and natural killer T cells. *Hepatol. Res.* **37**(Suppl. 3):S319–S326.
25. Yamagiwa, S., et al. 2008. Sustained response to interferon-alpha plus ribavirin therapy for chronic hepatitis C is closely associated with increased dynamism of intrahepatic natural killer and natural killer T cells. *Hepatol. Res.* **38**:664–672.
26. Van Wauwe, J.P., De Mey, J.R., and Goossens, J.G. 1980. OKT3: a monoclonal anti-human T lymphocyte antibody with potent mitogenic properties. *J. Immunol.* **124**:2708–2713.
27. Chang, T.W., Kung, P.C., Gingras, S.P., and Goldstein, G. 1981. Does OKT3 monoclonal antibody react with an antigen-recognition structure on human T cells? *Proc. Natl. Acad. Sci. U. S. A.* **78**:1805–1808.
28. Chatenoud, L., et al. 1990. In vivo cell activation following OKT3 administration. Systemic cytokine release and modulation by corticosteroids. *Transplantation.* **49**:697–702.
29. Soza, A., et al. 2005. Pilot study of interferon gamma for chronic hepatitis C. *J. Hepatol.* **43**:67–71.
30. Jo, J., et al. 2009. Analysis of CD8+ T-cell-mediated inhibition of hepatitis C virus replication using a novel immunological model. *Gastroenterology.* **136**:1391–1401.
31. Penna, A., et al. 2007. Dysfunction and functional restoration of HCV-specific CD8 responses in chronic hepatitis C virus infection. *Hepatology.* **45**:588–601.
32. Ohdan, H., et al. 2003. Intraoperative near-infrared spectroscopy for evaluating hepatic venous outflow in living-donor right lobe liver. *Transplantation.* **76**:791–797.
33. Tanaka, Y., Ohdan, H., Onoe, T., and Asahara, T. 2004. Multiparameter flow cytometric approach for simultaneous evaluation of proliferation and cytokine-secreting activity in T cells responding to allo-stimulation. *Immunol. Invest.* **33**:309–324.
34. Guo, J.T., Bichko, V.V., and Seeger, C. 2001. Effect of alpha interferon on the hepatitis C virus replicon. *J. Virol.* **75**:8516–8523.
35. Tanabe, Y., et al. 2004. Synergistic inhibition of intracellular hepatitis C virus replication by combination of ribavirin and interferon- alpha. *J. Infect. Dis.* **189**:1129–1139.
36. Yokota, T., et al. 2003. Inhibition of intracellular hepatitis C virus replication by synthetic and vector-derived small interfering RNAs. *EMBO Rep.* **4**:602–608.
37. Tsuge, M., et al. 2005. Infection of human hepatocyte chimeric mouse with genetically engineered hepatitis B virus. *Hepatology.* **42**:1046–1054.
38. Hiraga, N., et al. 2007. Infection of human hepatocyte chimeric mouse with genetically engineered hepatitis C virus and its susceptibility to interferon. *FEBS Lett.* **581**:1983–1987.
39. Kimura, T., et al. 2008. Establishment of an infectious genotype 1b hepatitis C virus clone in human hepatocyte chimeric mice. *J. Gen. Virol.* **89**:2108–2113.

Hepatology Research 2009; 39: 1159–1168 doi: 10.1111/j.1872-034X.2009.00566.x

Original Article

Effects of structural variations of *APOBEC3A* and *APOBEC3B* genes in chronic hepatitis B virus infection

Hiromi Abe,[1–3] Hidenori Ochi,[1–3] Toshiro Maekawa,[1,3] Tsuyoshi Hatakeyama,[2] Masataka Tsuge,[1,3,4] Shosuke Kitamura,[2] Takashi Kimura,[2] Daiki Miki,[2] Fukiko Mitsui,[2] Nobuhiko Hiraga,[1–3] Michio Imamura,[1–3] Yoshifumi Fujimoto,[1–3] Shoichi Takahashi,[1–3] Yusuke Nakamura,[5] Hiromitsu Kumada[6] and Kazuaki Chayama[1–3]

[1]*Laboratory for Digestive Diseases, Center for Genomic Medicine, RIKEN,* [2]*Department of Medicine and Molecular Science, Division of Frontier Medical Science, Programs for Biomedical Research, Graduate School of Biomedical Sciences,* [3]*Liver Research Project Center,* [4]*Natural Science Center for Basic Research and Development, Hiroshima University, Hiroshima,* [5]*Center for Genomic Medicine, RIKEN, Kanagawa, and* [6]*Department of Hepatology, Toranomon Hospital, Tokyo, Japan*

Aim: Human APOBEC3 deaminases induce G to A hypermutation in nascent DNA strand of hepatitis B virus (HBV) genomes and seem to operate as part of the innate antiviral immune system. We analyzed the importance of APOBEC3A (A3A) and APOBEC3B (A3B) proteins, which are potent inhibitors of adeno-associated-virus and long terminal repeat (LTR)-retrotransposons, in chronic HBV infection.

Methods: We focused on the common deletion polymorphism that spans from the 3′ part of *A3A* gene to the 3′ portion of *A3B* gene. An association study was carried out in 724 HBV carriers and 469 healthy control subjects. We also analyzed hypermutated genomes detected in deletion and insertion (non-deletion) homozygous patients to determine the effect of *APOBEC3* gene deletion. Further, we performed functional analysis of *A3A* gene by transient transfection experiments.

Results: The association study showed no significant association between deletion polymorphism and chronic HBV carrier state. Context analysis also showed a negligible effect for the deletion. Rather, mild liver fibrosis was associated with *APOBEC* gene deletion homozygosity, suggesting that *A3B* deletion is not responsible for chronic HBV infection. Functional analysis of A3A showed that overexpression of *A3A* induced hypermutation in HBV genome, although the levels of hypermutants were less than those introduced by *A3G*. However, overexpression of *A3A* did not decrease replicative intermediates of HBV.

Conclusion: These results suggest that A3A and A3B play little role in HBV elimination through anti-viral defense mechanisms. The significance of hypermutation induced by A3A should be investigated further.

Key words: APOBEC3A, APOBEC3B, APOBEC3G, deaminase, hypermutation, structural variation

INTRODUCTION

APOBEC3 CYTIDINE DEAMINASE family consists of at least seven tandem arrayed genes *APOBEC3A (A3A), A3B, A3C, A3DE, A3F, A3G,* and *A3H* on chromosome 22.[1,2] The anti-viral effect of A3G was initially identified in 2002 when it was found to inhibit the replication of human immunodeficiency virus (HIV).[3] Similarly, A3F, A3B and A3DE have been reported to inhibit HIV replication.[4–8]

APOBEC3 proteins also act on many other viruses such as simian immunodeficiency virus,[9] adeno-associated virus[10] and retrotransposons.[11–13] With regard to hepatitis B virus (HBV), A3G was also reported to inhibit HBV replication and induction of hypermutation, although the significance of the latter on viral inactivation is still controversial.[14–23] Among the APOBEC3 family members, A3B, A3C, A3G and A3F have been

Correspondence: Professor Kazuaki Chayama, Department of Medical and Molecular Science, Division of Frontier Medical Science, Programs for Biomedical Research, Graduate school of Biomedical Science, Hiroshima University, 1-2-3 Kasumi, Minami-ku, Hiroshima 734-8551, Japan. Email: chayama@hiroshima-u.ac.jp
Received 15 April 2009; revision 17 May 2009; accepted 18 May 2009.

extensively analyzed in these reports for induction of hypermutation and inhibition of replication of HBV. In contrast, the function of A3A on HBV has not been evaluated despite its potent inhibitory effects on adeno-associated virus and retrotransposons.[9–13] Recently, Henry *et al.*[24] reported that, among the APOBEC3 family, A3A is the most efficient editor in induction of hypermutation in the HBV genome. This finding is not consistent with the previous reports. However, the relationship between genomic DNA editing by A3A and its effect on HBV replication have not been elucidated. This background prompted us to examine the effects of A3A on HBV replication and induction of hypermutation.

A recent study[25] identified a common deletion polymorphism of *APOBEC* gene spanning from the 3′ end of *A3A* gene to the 3′ portion of *A3B* gene (the segment extending from exon 5 of *A3A* to exon 8 of *A3B* was removed by the deletion, positions 37, 683, 131–37, 712, 716 on chromosome 22). The deletion results in complete elimination of the *A3B* coding region and the resultant fusion gene has a protein sequence identical to A3A, but has 3′ untranslated region of A3B. This polymorphism might modulate the expression levels of A3A peptide because the transcription levels and stability of this fusion mRNA could be altered by replacement of the 3′ untranslated region sequences. Analyzing the association between this deletion polymorphism and chronic HBV infection should clarify the effect of *A3B* on the establishment of chronic HBV carrier state.

The aims of the present study were to determine the association between *APOBEC3* gene deletion polymorphism and chronic HBV infection and the effect of *A3A*, which might be up- or down-regulated by the deletion polymorphism, on HBV replication and induction of hypermutation, by *in-vitro* overexpression experiments.

PATIENTS AND METHODS

Study subjects

BLOOD SAMPLES WERE obtained from 724 patients with chronic HBV infection at the hospitals of the Hiroshima Liver Study Group (http://home.hiroshima-u.ac.jp/naika1/hepatology/english/study.html) and Toranomon hospital. We also collected 469 control samples from healthy individuals who agreed to join the BioBank Japan Project at the Institute of Medical Science, the University of Tokyo. The study protocols were approved by the ethics committees of the University of Tokyo and the Center for Genomic Medicine, Riken. All participants were ethnically Japanese and provided written informed consent. Histological activity and fibrosis was assessed in liver biopsy specimens by the Metavir score.[26]

HBV markers

We measured DNA polymerase by the method of Robinson *et al.*[27] The quantity of HBV DNA was assessed by the following tests. Quantiplex HBV DNA probe assay (Chiron Corporation, Emeryville, CA), PCR (Amplicor Cobas TaqMan HBV Auto; Roche Molecular Diagnostic, Basel), transcription mediated amplification (TMA) assay (Fujirevio Diagnostic, Tokyo). The level of HBV in serum was assessed as high or low according to the following criteria (< 200 or ≥ 200 for DNA polymerase, < 200 or ≥ 200 for probe assay, < 6.0 or ≥ 6.0 for PCR assay, < 6.0 or ≥ 6.0 for TMA assay).

HBV-e antigen (HBeAg) and HBV-e antibody (HBeAb) were measured by commercially available chemiluminescent enzyme immunoassay kit (Abbott Laboratories, Chicago, IL). The cut off levels were 1.0 (cut off index) for HBeAg and 70% for HBeAb.

Genotyping

First, we genotyped genomic samples of 94 individuals by the PCR assay using the Deletion and Insertion specific primer sets reported by Kidd *et al.*[25] Since we observed some non-specific amplification, which was confirmed by sequencing analysis, we used the invader probes,[28] which specifically recognize *A3A* and *A3B*. These probes were designed and synthesized by Third Wave Technologies (Madison, WI). Deletion and two-insertion (non-deletion) PCR assays were performed separately as described previously,[25] then pooled (Deletion : Insertion1 : Insertion2 = 3:1:1), and subjected to Invader assay.

Cell culture and transfection

Human liver cancer cell line, HepG2, was purchased from RIKEN Cell Bank (Tsukuba). The cells were cultured in Dulbecco's modified Eagle's medium supplemented with 10% fetal bovine serum at 37°C under 5% CO_2. Cells were seeded to semi-confluence in six-well tissue culture plates. Transient transfection experiments were performed using TransIT-LT1 (Mirus, Madison, WI) according to the instructions provided by the supplier.

Plasmid construction

The expression vector for hemagglutinin (HA)-tagged human A3G was kindly provided by Dr. Takaori (Kyoto University).[29] We constructed A3A cDNA expression

plasmid by cloning DNA fragment, which was amplified by PCR from cDNA obtained from lymphocytes of a deletion homozygous patient, into pcDNA3.1/nV5-DEST (Invitrogen, Carlsbad, CA). Construction of the wild-type HBV 1.4 genome length plasmid, pTRE-HB-wt was described previously (Tsuge *et al.*;[30] GenBank accession no. AB206816).

Analysis of core-associated HBV DNA

The cells were harvested 4 days after transfection and lysed with 250 μl lysis buffer [10 mM Tris/HCl, pH 7.4, 140 mM NaCl and 0.5% (v/v) NP-40]. The lysate was then centrifuged for 2 min at 15 000 × *g*. The core particles were immunoprecipitated from the supernatant by mouse anti-core monoclonal antibody (anti-HBc determinant α, Institute of Immunology, Tokyo). Genomic DNA was separated from the core particles by SDS/proteinase K digestion followed by phenol extraction and ethanol precipitation. Quantitative analysis was performed using the above HBV DNA by RT-PCR using the RT-PCR system (Applied Biosystems, Foster City, CA). The primers and the probe used were described previously.[31] The real-time PCR was performed in a 25-μl reaction volume containing 2×TaqMan Gene Expression Master Mix, 0.9 μM of each primer, 0.25 μM probe and 1 μl DNA solution. The thermal profile was 50°C for 2 min, 95°C 10 min, followed by 40 cycles of amplification (denaturation at 95°C for 15 sec, annealing at 55°C for 30 sec and extension at 62°C for 90 sec).

Analysis of hypermutated HBV genomes by 3D-RT-PCR

Hypermutated genomes were detected and quantified by modified 3DRT-PCR using the primers, probe and reagents described previously.[31] The thermal profile was 50°C for 2 min, 95°C for 10 min followed by initial denaturation at 85°C for 20 min and 45 cycles of amplification (denaturation at 85°C for 15 sec, annealing at 50°C for 30 sec and extension at 62°C for 90 sec).

Detection of A3A-A3B fusion mRNA by RT-PCR

We extracted total RNA from lymphocytes of each allele patients using RNeasy Mini Kit (Qiagen, Hilden) and reverse-transcribed using ReverTra Ace (TOYOBO, Osaka) with random primer in accordance with the instructions supplied by the manufacturer. We then amplified cDNAs by 35 cycles of PCR using primers specific for exon 1 of *A3A* and 3′-untranslated region of *A3B* in a 25μl reaction volume containing 1 × KOD-Plus buffer [0.3 μM each primers, 0.2 mM $MgSO_4$, 1 μl DNA solution and 1 unit of KOD-Plus (TOYOBO Co.)]. The thermal profile was initial denaturation at 98°C for 2 min, followed by 35 cycles of amplification (denaturation at 98°C for 15 sec, annealing at 58°C for 15 sec and extension at 68°C for 60 sec). Nucleotide sequences of the amplified fusion cDNA sequences were confirmed by direct sequencing.

Western blot analysis

Cell lysates prepared as described above were separated by sodium dodecyl sulfate polyacrylamide electrophoresis on a 12% poly acrylamide gel and transferred to polyvinylidene fluoride (Pall Corporation, Pensacola, FL). The membranes were incubated with anti-V5 (Invitrogen), anti-hemagglutinin fusion epitope monoclonal anti-body (Roche) or with anti-β-actin monoclonal antibody (Sigma-Aldrich, St Louis, MO) followed by incubation with horseradish peroxidase-conjugated sheep anti-mouse antibody (GE Healthcare UK, Buckinghamshire). We detected signals using the ECL system (GE Healthcare).

Nucleotide sequencing analysis of hypermutated HBV genomes by 3D-PCR, cloning and nucleotide sequencing

We analyzed hypermutated HBV DNA genomes obtained from serum samples of each genotype patient by 3D PCR (denaturation at 85°C) and cloning and sequencing. The amplified DNA fragments were cloned into pGEM T Easy vector (Promega Corporation, Madison, WI) by TA cloning. Nucleotide sequences were determined using BigDye Terminator v3.1 Cycle Sequencing Kit (Applied Biosystems). The nucleotide sequences were compared with those obtained by direct sequencing of amplified PCR products by normal PCR protocol.

Statistical analysis

The allele frequencies was calculated and fit to Hardy-Weinberg equilibrium was tested by the chi-square test between cases and controls using Excel software (Microsoft, Redmond, WA).[32] We also compared differences in allele frequency and genotype distribution of the deletion between cases and controls with χ^2-test. Continuous data were compared by analysis of variance (ANOVA). Differences in categorical data were analyzed by the χ^2-test. Differences in core-associated HBV and hypermutated HBV genomes per 1×10^4 copies of HBV genomes, were analyzed by Student's *t*-test.

Table 1 Characteristics of subjects

	Patients	Control	*P*-value
Number of patients	724	469	–
Sex			NS
Male	499	373	
Female	224	95	
Age (years)	53.1 (20.6–86.4)	55 (18–93)	NS
ALT	66 (5–3634)	–	–
Fibrosis stage		–	–
F0	13		
F1	80		
F2	149		
F3	114		
F4	46		
Activity		–	–
A0	1		
A1	50		
A2	125		
A3	47		
Platelet ($\times 10^4/mm^3$)	16.5 (2.2–29.8)	–	–
HBV DNA		–	–
High	137		
Middle	108		
Low	156		
HBeAg/HBeAb		–	–
+/–	207		
–/+	184		
Hepatocellular carcinoma	65	–	–

Data are number of patients or median (range) values. Differences in age between case and control were compared by Mann–Whitney *U*-test. The sex ratio was analyzed by the χ^2-test. ALT, alanine aminotransferase; HBVeAb, hepatitis B virus e antibody; HBVeAg, hepatitis B virus e antigen; NS, not significant.

RESULTS

Association between chronic HBV carriers, clinical parameters and the APOBEC3 gene deletion

TABLE 1 SUMMARIZES the clinicopathological features of the patients and control subjects. If A3B contributes to the prevention of chronic HBV infection, there should be an association between chronic HBV carrier state and *APOBEC* gene deletion polymorphism. However, we did not find any association between the two (Table 2). Furthermore, all clinical parameters, with the exception of the extent of liver fibrosis associated with chronic HBV, did not associate with the polymorphism (Tables 3,4). Advanced histopathological stages were associated with insertion homozygosity. These findings also suggest that A3B does not play any important role in anti-viral immunity in the development of chronic HBV infection.

Table 2 Case-control analysis of *APOBEC3B* deletion

	Frequency (%)		Additive mode		
	Ins	Del	*P*-value	OR	95% CI
HBV ($n = 724$)	0.709	0.291	0.599	0.964	0.624–1.489
Control ($n = 469$)	0.719	0.281			

P-values were calculated from case-control analysis by χ^2-test. OR, odds ratio; CI, confidence interval; Del, deletion homozygote; Ins, insertion homozygote.

Table 3 Correlation between deletion and clinical parameters

	Genotype			*P*-value
	I/I	I/D	D/D	
Genotype frequency	0.50	0.42	0.08	NS
Age (years)	54.0 ± 12.8	52.0 ± 12.6	50.4 ± 13.3	NS
ALT	169.0 ± 320.6	149.5 ± 322.9	196.8 ± 309.3	NS
Platelets ($\times 10^4/mm^3$)	16.8 ± 5.2	16.6 ± 6.1	17.0 ± 5.8	NS

Data are number of patients or mean ± SD. Age, ALT and platelet count were compared by ANOVA. ALT, alanine aminotransferase; D/D, deletion homozygote; H, heterozygote; I/I, insertion homozygote; NS, not significant.

Context analysis of hypermutated genomes obtained from deletion homozygous and insertion homozygous patients

The amount of hypermutated genomes was not analyzed in this study because it is known to fluctuate during the clinical course.[33] Instead, we searched for the target context of G to A mutation in hypermutated HBV genomes using serum obtained from patients with deletion homozygotes and with insertion homozygotes. As shown Figure 1, multiple G to A hypermutations were observed in deletion homozygote and insertion homozygote patients. The results of context analysis showed no significant difference between the contexts obtained from deletion homozygotes and those form non-deletion homozygotes (Fig. 2). In fact, the preferred contexts were similar in all three deletion homozygous patients and one insertion homo patient (DD1-3 and II1 in Fig. 2) but slightly different from those of the remaining two (II2 and II3). These results suggest that the effect of deletion is not strong in these preferred context patterns.

Detection of A3A-A3B fusion mRNA

We then analyzed whether the resultant *A3A* and A3B fusion was actually transcribed. We designed primers specific for exon 1 of *A3A* and the 3′-untranslated region

Table 4 Association of clinical parameters and *APOBEC* gene polymorphism (categorical data)

	Genotype frequency				Additive mode	I/I vs I/D, D/D	D/D vs I/I, I/D
	I/I	I/D	D/D				
Sex (Male/Female)				*P* value	0.76	0.85	0.30
Male ($n = 328$)	154 (0.47)	143 (0.44)	31 (0.09)	OR	0.75	1.03	0.72
Female ($n = 166$)	78 (0.47)	74 (0.45)	14 (0.08)	95% CI	0.40–1.41	0.75–1.41	0.40–1.33
Fibrosis stage (F0-F1/F2-F4)				*P* value	0.0054	0.0019	0.48
F0-F1 ($n = 62$)	22 (0.35)	34 (0.55)	6 (0.10)	OR	0.51	0.47	0.74
F2-F4 ($n = 187$)	95 (0.51)	77 (0.41)	15 (0.08)	95% CI	0.21–1.24	0.30–0.76	0.31–1.73
Activity (A0-A1/A2-A3)				*P* value	0.31	0.46	0.30
A0-A1 ($n = 51$)	22 (0.43)	23 (0.45)	6 (0.12)	OR	0.56	0.80	0.60
A2-A3 ($n = 168$)	81 (0.48)	75 (0.45)	12 (0.07)	95% CI	0.20–1.56	0.45–1.44	0.22–1.60
HBV DNA (High/Low)				*P* value	0.12	0.12	0.47
High ($n = 194$)	82 (0.42)	94 (0.48)	18 (0.09)	OR	0.66	0.73	0.77
Low ($n = 206$)	103 (0.50)	88 (0.43)	15 (0.07)	95% CI	0.32–1.40	0.49–1.09	0.38–1.57
HBeAg/HBeAb ((+/−)/(−/+))				*P* value	0.52	0.34	0.84
+/− ($n = 207$)	89 (0.43)	99 (0.48)	19 (0.09)	OR	0.96	0.82	1.07
−/+ ($n = 184$)	88 (0.48)	78 (0.42)	18 (0.10)	95% CI	0.47–1.95	0.55–1.23	0.54–2.11
HCC				*P* value	0.85	0.89	0.64
(−) ($n = 648$)	323 (0.50)	266 (0.41)	59 (0.09)	OR	0.73	1.04	0.69
(+) ($n = 65$)	34 (0.52)	31 (0.47)	0 (0.00)	95% CI	0.25–2.13	0.62–1.73	0.24–1.98

ALT, alanine aminotransferase CI, confidence interval; D/D deletion homozygote; H, heterozygote; HBVeAg, hepatitis B virus e antibody; HBVeAg, hepatitis B virus e antigen; HCC, hepatocellular carcinoma; I/I, insertion homozygote; OR, odds ratio.

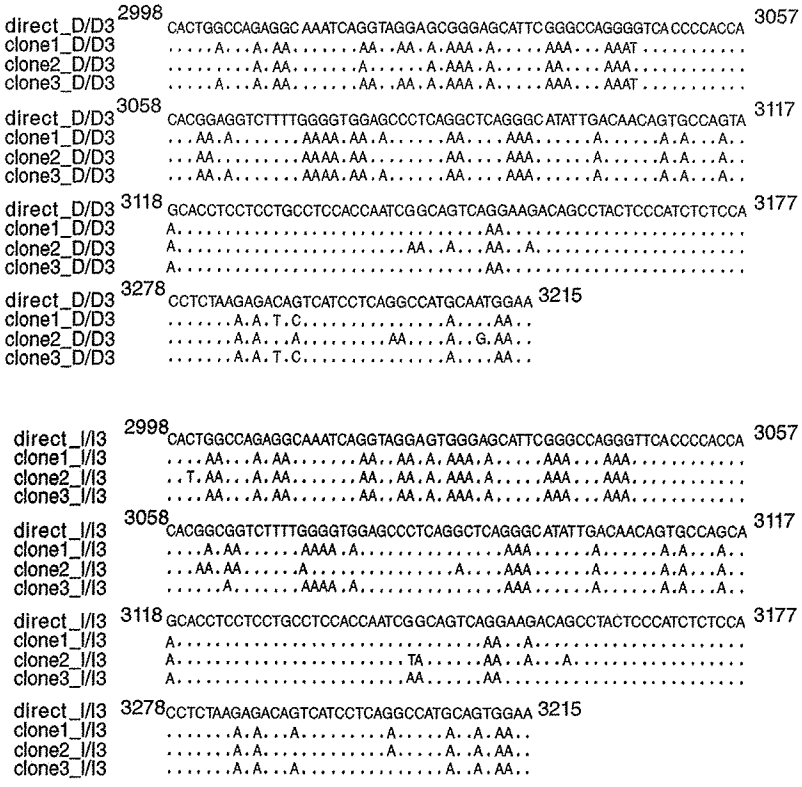

Figure 1 Nucleotide sequences of hypermutated genomes detected from deletion homozygous and insertion homozygous patients. Nucleotide sequences of 3D-PCR amplified hebatitis B virus (HBV) DNA clones are compared with those obtained by usual PCR and direct sequencing. Upper panel, nucleotide sequences obtained from a deletion homozygous patient. Lower panel, nucleotide sequences obtained from a homozygous patient. Nucleotide numbers are those from GenBank accession no. AB206816.

of *A3B*, and performed RT-PCR using cDNAs obtained from patients of each genotype. We obtained amplified DNA fragments of expected size only from deletion homozygotes and heterozygotes (Fig. 3). These results confirmed the transcription of the fusion mRNA with the coding region of *A3A* and the 3′ untranslated region of *A3B*.

Inhibition of HBV replication and induction of hypermutation by A3A

We then analyzed the antiviral effect and induction of hypermutation by A3A. Although the expression of both A3A and A3G was confirmed by western Blot analysis (Fig. 4A), transient expression of A3A did not reduce the amount of the core-associated HBV DNA in HepG2 cells (Fig. 4B). However, A3A transfection increased the hypermutated genomes of HBV in a dose-dependent manner albeit the level of induction was much lower than that observed when transfected with A3G. These results suggest that A3A has negligible anti-viral effect although it induces hypermutation of HBV genomes.

DISCUSSION

THE MAIN FINDINGS of the present study were: (i) no association between *APOBEC3* deletion and chronic HBV infection (Table 2). (ii) Mild liver fibrosis and low alanine amino transferase (ALT) levels were associated with APOBEC gene deletion homozygous genotype. (iii) The absence of *A3B* is not responsible for chronic HBV carrier status, although A3B is known as a potent inhibitor of adeno-associated virus and retrotransposons.[12] This suggests different antiviral activities for APOBEC proteins against viruses and that A3B plays little role in inhibition of HBV. (iv) The preferred context analysis showed no differences between insertion homozygotes and deletion homozygotes. Only one of the six patients examined showed different context pattern (Fig. 2). These results suggest that A3B protein has only small effect on the formation of hypermutated genomes in the serum of chronic carriers. The protein has been reported to induce hypermutation on the negative and positive strands of HBV.[18] However, our results showed that the effect of *A3B* is almost negligible in

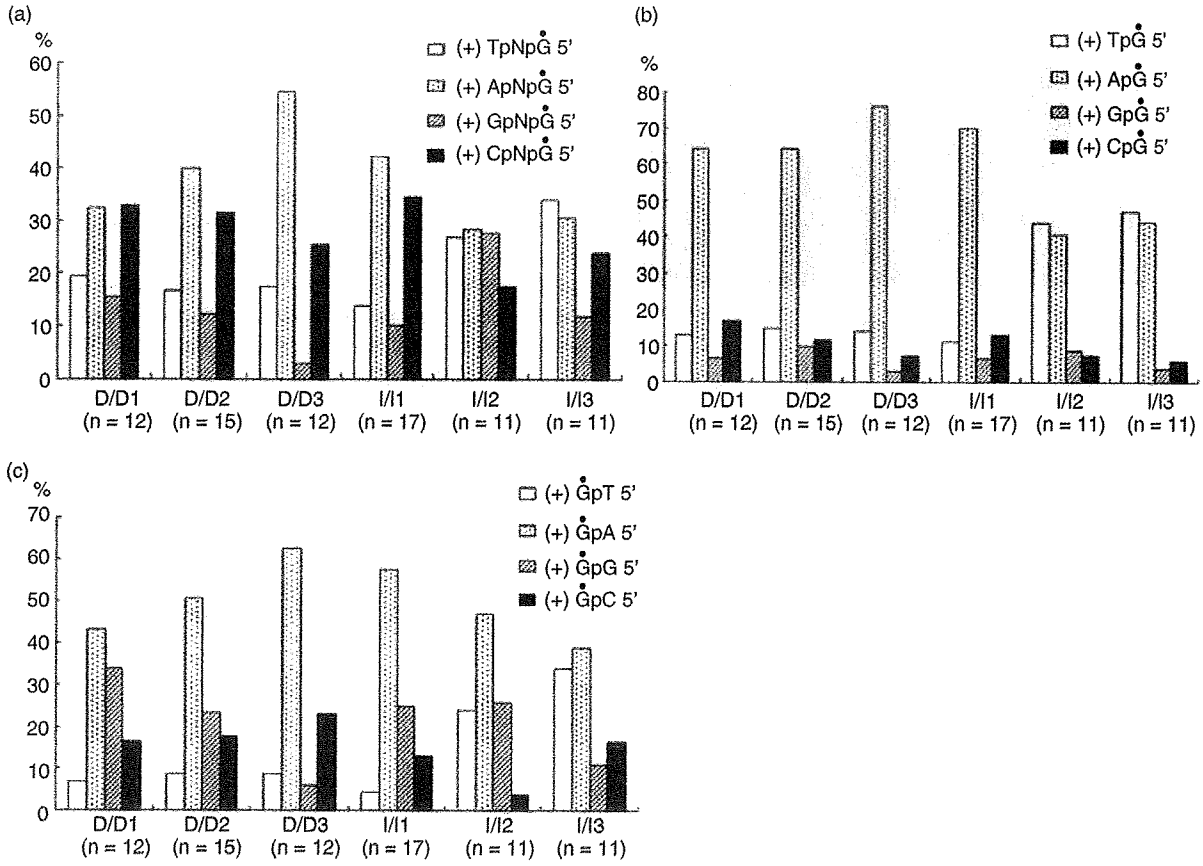

Figure 2 Context analysis of hypermutated genomes from deletion homozygous and insertion homozygous patients. Context of G to A hypermutation in hypermutated genome clones obtained from three deletion homozygous patients (D/D1, D/D2 and D/D3) and three insertion homozygous patients (I/I1, I/I2 and I/I3) were analyzed. Numbers after each patient represent the number of clones analyzed in each patient. (a) Two letters up-stream, (b) one letter upstream and (c) one letter downstream of mutated G residue were analyzed.

chronic HBV carriers compared to that of A3G. It is assumed that the other APOBEC3 family proteins mainly induce hypermutation of HBV genomes in HBV carriers to compensate for the function of deleted A3B. It is also assumed that the expression pattern of the remaining six APOBEC3 proteins is different from patient to patient.

As discussed above, our results suggest that A3B protein has almost no effect on prevention of chronic HBV infection and induction of hypermutation. It is thus assumed that A3B is not part of the innate anti-viral immune system against HBV. This is consistent with the finding that deletion is commonly seen in normal populations[25] irrespective of HBV carrier rates. Other association studies are required to clarify the role of A3B protein on other pathogens. The functional relevance of other APOBEC3 proteins on HBV infection as anti-viral immunity should be clarified further.

We also found that A3A protein induced hypermutation on the negative strand of HBV. However, the level of induction of hypermutation was much less than that of A3G (Fig. 4). Recent reports showed quite different effects for *A3A* on induction of hypermutation on HBV genomes. Henry *et al.*[24] reported that A3A is the most efficient editor of seven APOBEC3 proteins. In contrast, Zang *et al.*[23] did not detect induction of hypermutation on HBV. Although these different results might come from different cell lines and conditions used in each experiment, our results clearly showed that *A3A* induced hypermutation on the negative strand of HBV genome.

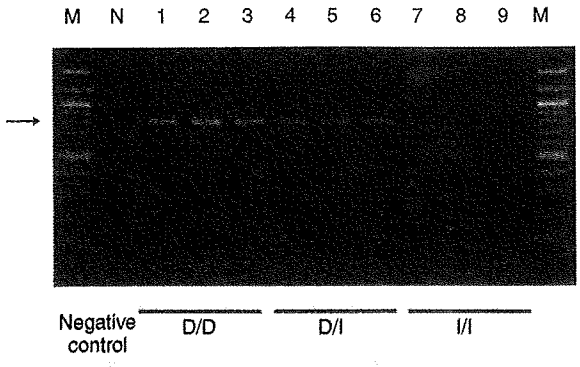

Figure 3 Detection of A3A-A3B fusion mRNA by PCR. A3A-A3B fusion mRNA was amplified by PCR using primers specific to A3A and A3B (see Materials and Methods) and detected by agarose gel electrophoresis. Lanes 1–3 are those from deletion homozygous patients, lanes 4–6 are from heterozygous patients and 7–9 are from insertion homozygous patients. M, molecular weight size marker (1 kb DNA Ladder; New England BioLabs, Ipswich, MA), N, negative control.

The deletion of APOBEC gene spans from 3′ end of the *A3A* gene to the 3′ portion of the *A3B* gene. This deletion results in the formation of a fusion gene that has *A3A* amino acid sequence and *A3B* 3′ untranslated region. The expression level of this protein may be different from the undeleted *A3A* due to different stability of RNA or different transcription levels. The results of context analysis also indicated that the effect of this alteration of expression levels of *A3A* is almost negligible compared with A3G. This is consistent with our results that showed lower levels of induction of hypermutation on HBV genome by *A3A* compared with *A3G*.

Our results indicated that the effect of both *A3A* and *A3B* is not significant in the development and progression of chronic hepatitis B. The two proteins also have only little influence on the hypermutation state of HBV in chronic HBV carriers. The results also showed higher induction levels of hypermutation by *A3G* than by *A3A*.

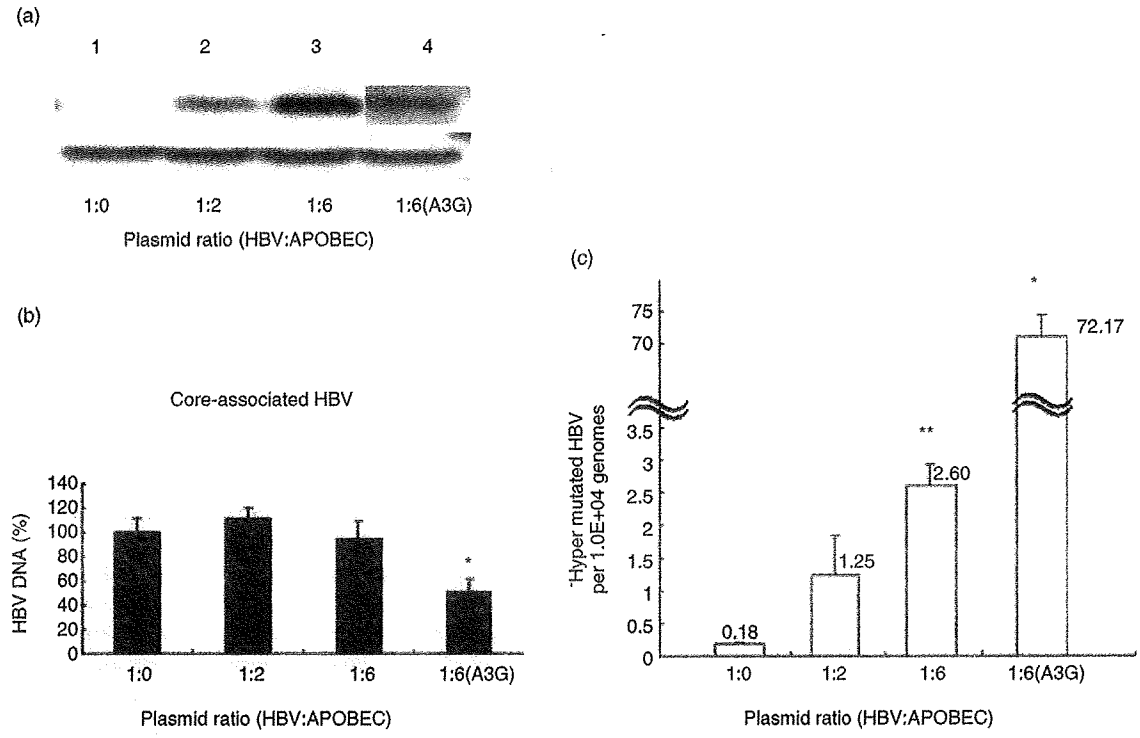

Figure 4 Analysis of inhibition of HBV replication and induction of hypermutation by A3A. HepG2 cells were transiently transfected with expression plasmid of A3A together with 1.4 genome length hepatitis B virus (HBV) expression vector. The indicated amounts of HBV and A3A (1:0, 1:2, 1:6) or A3G (1:6) expression plasmids were transfected into HepG2 cells. All experiments were performed more than twice with similar results. (a) APBEC3 gene expression levels were detected by western blot analysis. (b) The amounts of core associated replicative intermediates of HBV were measured by RT-PCR. (c) Quantitative measurement of hypermutated genomes by 3D real-time PCR. Data in (B) and (C) are mean ± SD. $*P < 0.05$; $**P < 0.01$

Sufficient evidence indicates that *A3G* has anti-viral effects on HBV,[14–17] suggesting that some but not all APOBEC3 proteins operate as part of the anti-viral immune system against HBV infection. Further study is needed to clarify the functional role of each APOBEC3 protein for innate anti-viral immunity in chronic HBV infection.

ACKNOWLEDGMENT

THE AUTHORS THANK Rie Akiyama, Yoshie Yoshida, Tomomi Murai, Kazuyo Hattori, Mariko Shiota, and Takako Yokogi for the excellent technical assistance, and Yuko Nagai, Junko Sakamiya and Aya Furukawa for the secretarial assistance. We are also grateful to members of Hiroshima Liver Study Group and The Rotary Club of Osaka-Midosuji Direct 2660 Rotary International in Japan for supporting our study. Part of this work was carried out at the Analysis Center of Life Science, Hiroshima University. This work was supported in part by Grants-in-Aid for scientific research and development from the Ministry of Health, Labor and Welfare, Government of Japan.

REFERENCES

1 Jarmuz A, Chester A, Bayliss J *et al.* An anthropoid-specific locus of orphan c to u rnaediting enzymes on chromosome 22. *Genomics* 2002; 79: 285–96.
2 Wedekind JE, Dance GS, Sowden MP, Smith HC. Messenger RNA editing in mammals: new members of the APOBEC family seeking roles in the family business. *Trends Genet* 2003; 19: 207–16.
3 Sheehy AM, Gaddis NC, Choi JD, Malim MH. Isolation of a human gene that inhibits HIV-1 infection and is suppressed by the viral Vif protein. *Nature* 2002; 418: 646–50.
4 Bishop KN, Holmes RK, Sheehy AM, Davidson NO, Cho SJ, Malim MH. Cytidine deamination of retroviral DNA by diverse APOBEC proteins. *Curr Biol* 2004; 14: 1392–96.
5 Liddament MT, Brown WL, Schumacher AJ, Harris RS. APOBEC3F properties and hypermutation preferences indicate activity against HIV-1 in vivo. *Curr Biol* 2004; 14: 1385–91.
6 Wiegand HL, Doehle BP, Bogerd HP, Cullen BR. A second human antiretroviral factor, APOBEC3F, is suppressed by the HIV-1 and HIV-2 Vif proteins. *EMBO J* 2004; 23: 2451–8.
7 Zheng YH, Irwin D, Kurosu T, Tokunaga K, Sata T, Peterlin BM. Human APOBEC3F is another host factor that blocks human immunodeficiency virus type 1 replication. *J Virol* 2004; 78: 6073–6.
8 Dang Y, Wang X, Esselman WJ, Zheng YH. Identification of APOBEC3DE as another antiretroviral factor from the human APOBEC family. *J Virol* 2006; 80: 10522–33.
9 Cullen BR. Role and mechanism of action of the APOBEC3 family of antiretroviral resistance factors. *J. Virol* 2006; 80: 1067–76.
10 Chen H, Lilley CE, Yu Q *et al.* APOBEC3A is a potent inhibitor of adeno-associated virus and retrotransposons. *Curr Biol* 2006; 16: 480–5.
11 Bogerd HP, Wiegand HL, Doehle BP, Lueders KK, Cullen BR. APOBEC3A and APOBEC3B are potent inhibitors of LTR-retrotransposon function in human cells. *Nucleic Acids Res* 2006; 34: 89–95.
12 Bogerd HP, Wiegand HL, Hulme AE *et al.* Cellular inhibitors of long interspersed element 1 and Alu retrotransposition. *Proc Natl Acad Sci USA* 2006; 103: 8780–5.
13 Chen H, Lilley CE, Yu Q *et al.* APOBEC3A is a potent inhibitor of adeno-associated virus and retrotransposons. *Curr Biol* 2006; 16: 480–5.
14 Turelli P, Mangeat B, Jost S, Vianin S, Trono D. Inhibition of hepatitis B virus replication by APOBEC3G. *Science* 2004; 303: 1829.
15 Rösler C, Köck J, Malim MH, Blum HE, von Weizsäcker F. Comment on "inhibition of hepatitis B virus replication by APOBEC3G". *Science* 2004; 305: 1403a.
16 Turelli P, Jost S, Mangeat B, Trono D. Response to comment on "inhibition of hepatitis B virus replication by APOBEC3G". *Science* 2004; 305: 1403b.
17 Noguchi C, Ishino H, Tsuge M *et al.* G to A hypermutation of hepatitis B virus. *Hepatology* 2005; 41: 626–33.
18 Suspène R, Guétard D, Henry M, Sommer P, Wain-Hobson S, Vartanian JP. Extensive editing of both hepatitis B virus DNA strands by APOBEC3 cytidine deaminases in vitro and in vivo. *Proc Natl Acad Sci* 2005; 102: 8321–6.
19 Bonvin M, Achermann F, Greeve I *et al.* Interferon-inducible expression of APOBEC3 editing enzymes in human hepatocytes and inhibition of hepatitis B virus replication. *Hepatology* 2006; 43: 1364–74.
20 Xu R, Zhang X, Zhang W, Fang Y, Zheng S, Yu XF. Association of human APOBEC3 cytidine deaminases with the generation of hepatitis virus B x antigen mutants and hepatocellular carcinoma. *Hepatology* 2007; 46: 1810–20.
21 Jost S, Turelli P, Mangeat B, Protzer U, Trono D. Induction of antiviral cytidine deaminases does not explain the inhibition of hepatitis B virus replication by interferons. *J Virol* 2007; 81: 10588–96.
22 Bonvin M, Greeve J. Effects of point mutations in the cytidine deaminase domains of APOBEC3B on replication and hypermutation of hepatitis B virus in vitro. *J Gen Virol* 2007; 88: 3270–4.
23 Zhang W, Zhang X, Tian C *et al.* Cytidine deaminase APOBEC3B interacts with heterogeneous nuclear ribonucleoprotein K and suppresses hepatitis B virus expression. *Cell Microbiol* 2008; 10: 112–21.

24 Henry M, Guétard D, Suspène R, Rusniok C, Wain-Hobson S, Vartanian JP. Genetic editing of HBV DNA by monodomain human APOBEC3 cytidine deaminases and the recombinant nature of APOBEC3G. *PLoS ONE* 2009; 4: e4277.
25 Kidd JM, Newman TL, Tuzun E, Kaul R, Eichler EE. Population stratification of a common APOBEC gene deletion polymorphism. *PLoS Genet* 2007; 3: e63.
26 Bedossa P, Poynard T. An algorithm for the grading of activity in chronic hepatitis C. The METAVIR Cooperative Study Group. *Hepatology* 1996; 24: 289–93.
27 Price PM, Banerjee R, Jeffrey AM, Acs G. The mechanism of inhibition of hepatitis B virus replication by the carbocyclic analog of 2′-deoxyguanosine. *Hepatology* 1992; 16: 8–12.
28 Ohnishi Y, Tanaka T, Ozaki K, Yamada R, Suzuki H, Nakamura Y. A high-throughput SNP typing system for genome-wide association studies. *J Hum Genet* 2001; 46: 471–7.
29 Kobayashi M, Takaori-Kondo A, Shindo K, Abudu A, Fukunaga K, Uchiyama T. APOBEC3G targets specific virus species. *J Virol* 2004; 78: 8238–44.
30 Tsuge M, Hiraga N, Takaishi H *et al.* Infection of human hepatocyte chimeric mouse with genetically engineered hepatitis B virus. *Hepatology* 2005; 42: 1046–54.
31 Noguchi C, Hiraga N, Mori N *et al.* Dual effect of APOBEC3G on hepatitis B virus. *J Gen Virol* 2007; 88: 432–40.
32 Nielsen DM, Ehm MG, Weir BS. Detecting marker-disease association by testing for Hardy-Weinberg disequilibrium at a marker locus. *Am J Hum Genet* 1998; 63: 1531–40.
33 Noguchi C, Imamura M, Tsuge M *et al.* G to A hypermutation in hepatitis B virus and clinical course of patients with chronic hepatitis B. *J Inf Dis* 2009; 199: 1599–607.

MAJOR ARTICLE

G-to-A Hypermutation in Hepatitis B Virus (HBV) and Clinical Course of Patients with Chronic HBV Infection

Chiemi Noguchi,[1,2] Michio Imamura,[1,2] Masataka Tsuge,[1,2] Nobuhiko Hiraga,[1,2] Nami Mori,[1,2] Daiki Miki,[1,2] Takashi Kimura,[1,2] Shoichi Takahashi,[1,2] Yoshifumi Fujimoto,[1,2] Hidenori Ochi,[2,3] Hiromi Abe,[1,3] Toshiro Maekawa,[3] Chise Tateno,[2,4] Katsutoshi Yoshizato,[2,4] and Kazuaki Chayama[1,2,3]

[1]Department of Medicine and Molecular Science, Division of Frontier Medical Science, Programs for Biomedical Research, Graduate School of Biomedical Sciences, and [2]Liver Research Project Center, Hiroshima University, Hiroshima, [3]Laboratory for Liver Diseases, Single-Nucleotide Polymorphism Research Center, the Institute of Physical and Chemical Research, Yokohama, and [4]PhoenixBio, Higashihiroshima, Japan

Background. The apolipoprotein B messenger RNA editing enzyme, catalytic polypeptide–like family of cytidine deaminases induce G-to-A hypermutation in hepatitis B virus (HBV) genomes and play a role in innate antiviral immunity. The clinical relevance of this protein family is unknown.

Methods. We analyzed 33 instances in which 17 patients with chronic HBV infection experienced >2 increases of >100 IU/L in alanine aminotransferase (ALT) level; we used a quantitative differential DNA denaturation polymerase chain reaction assay to quantify the hypermutated HBV genomes observed during 21 of these 33 increases in ALT level.

Results. Of the 9 increases in ALT level that involved a >5-fold increase (relative to basal levels) in the number of hypermutated genomes observed, 8 were associated with a >2-log reduction in plasma HBV DNA level. In contrast, a corresponding decrease in plasma HBV DNA level was observed for only 1 of the 12 increases in ALT level that did not involve an increase in the number of hypermutated genomes ($P < .001$). Hepatitis B e antigen clearance was often observed in patients who experienced an increase in the number of hypermutated genomes. Interferon treatment induced hypermutation in HBV genomes in an animal model. However, there was no apparent increase in the number of hypermutated genomes among the majority of patients who received interferon therapy, probably because the number of hypermutated genomes had already increased prior to the initiation of therapy.

Conclusion. Our results suggest that a marked increase in the number of hypermutated genomes represents a strong immunological host response against the virus and is predictive of hepatitis B e antigen clearance and plasma HBV DNA level reduction.

Despite the availability of safe and effective vaccines for >2 decades, hepatitis B virus (HBV) infection is still a global health problem. Worldwide, >2 billion people are infected with HBV, and chronic HBV infection affects ~400 million people [1, 2]. It is estimated that >500,000 people die annually because of cirrhosis and/or hepatocellular carcinoma due to HBV infection [3].

Recent reports have shown that cellular cytosine deaminase (apolipoprotein B messenger RNA [mRNA] editing enzyme, catalytic polypeptide–like 3G [APOBEC3G]), packaged in human immunodeficiency virus type 1 (HIV-1), induces G-to-A hypermutation to a nascent reverse transcript of HIV-1 and reduces the infectivity of HIV, thus contributing in part to innate antiviral activity [4–8]. HIV-1 overcomes this innate defense barrier in T cells with HIV virion infectivity factor, a protein that specifically targets APOBEC3G to proteasomal degradation [9–12]. HIV-1 can infect resting CD4 T cells in lymphoid tissues but not those circulating in peripheral blood [13–16]. Resting CD4 T cells in peripheral blood are protected from HIV infection through the action of the deaminase-active

Received 30 August 2008; accepted 6 November 2008; electronically published 28 April 2009.

Potential conflicts of interest: none reported.

Financial support: Ministry of Education, Sports, Culture and Technology and Ministry of Health, Labor and Welfare (Grants-in-Aid for scientific research and development).

Reprints or correspondence: Kazuaki Chayama, MD, Dept. of Medical and Molecular Science, Div. of Frontier Medical Science, Programs for Biomedical Research, Graduate School of Biomedical Science, Hiroshima University, 1-2-3 Kasumi, Minami-ku, Hiroshima 734-8551, Japan (chayama@hiroshima-u.ac.jp).

The Journal of Infectious Diseases 2009; 199:1599–607

0022-1899/2009/19911-0007$15.00
DOI: 10.1086/598951

Table 1. Clinical profiles of 17 patients with chronic hepatitis B virus (HBV) infection who experienced >2 increases of >100 IU/L in alanine aminotransferase (ALT) level.

Patient	Sex	Age, years	ALT level, IU/L		Plasma HBV DNA level, log copies/mL	HBV serum marker status[a]		HBV subtype	Histologic result[b]	Receipt of IFN treatment
			Minimum	Maximum		HBeAg	HBeAb			
1	M	60	26	2000	8.1	+	−	C	F2, A2	Yes
2	M	31	22	230	8.2	+	−	C	F3, A2	Yes
3	F	23	14	313	8.7	+	−	C	F2, A2	Yes
4	M	22	16	846	6.9	+	−	C	F2, A1	Yes
5	F	42	10	100	7.8	+	−	C	L	No
6	F	33	21	748	8.8	+	−	C	F2, A3	Yes
7	M	23	22	339	8.4	+	−	C	L	Yes
8	F	54	22	108	6.7	−	+	C	F2, A2	No
9	M	44	17	512	9.6	+	−	C	F2, A3	No
10	M	27	39	115	8.8	+	−	C	F1, A1	Yes
11	M	36	16	452	3.8	+	−	C	F4, A3	Yes
12	M	20	21	1295	7.2	+	−	C	F2, A2	No
13	M	36	24	481	5.7	−	+	C	F2, A2	Yes
14	M	22	20	696	5.9	+	−	C	F1, A1	Yes
15	F	24	14	1544	7.7	+	−	C	F2, A2	Yes
16	M	35	10	1618	4.7	+	−	C	F2, A1	Yes
17	M	30	21	1655	6.7	+	−	C	L	Yes

NOTE. HBeAg, HBV e antigen; HBeAb, antibody against HBV e antigen; IFN, interferon; L, liver cirrhosis.

[a] Before increase in ALT level.

[b] Histologic evaluation of chronic hepatitis by use of the scoring system of Desmet et al. [29].

APOBEC3G [17]. Recent reports have shown that interferon (IFN)–α is a potent inducer of APOBEC3G [18–21]. It has also been reported that some of the HIV restriction exerted by APOBEC3G may be independent of its cytidine deaminase activity [17, 22–24].

We and others have reported the presence of small numbers of hypermutated genomes in serum samples obtained from HBV-infected patients [25–27]. Studies using HepG2 cell lines and primary human hepatocytes showed that such hypermutation is induced by the cytidine deaminase activity of the APOBEC family of proteins [27]. In our previous study, IFN induced little hypermutation in the HBV genome [27]. However, after extensive investigation supported by development of a quantitative analysis of hypermutation, we showed that both IFN-α and IFN-γ actually increase transcription of APOBEC3G mRNA in HepG2 cell lines and induce an increase in the number of hypermutated genomes [28]. We also showed that APOBEC3G induces hypermutation in HBV and reduces HBV replication levels in the absence of the deaminase activity. Thus, APOBEC3G has dual antiviral actions against HBV and is thought to be part of the host defense mechanisms, as has been shown for HIV infection. Although it is assumed that APOBEC3G is important in the host anti-HBV defense system, little is known about the clinical importance of this enzyme, because there are no methods available for the precise quantification of small amounts of hypermutated genomes.

Using a method that can measure small amounts of hypermutated genomes (differential DNA denaturation polymerase chain reaction [3D-PCR] combined with TaqMan PCR [28]), we analyzed fluctuations in the number of hypermutated genomes observed in patients with chronic HBV infection who experienced increased alanine aminotransferase (ALT) levels. The study group included patients who received IFN treatment and patients who did not.

METHODS

Patients. From 2002 through 2006 at Hiroshima University Hospital (Hiroshima, Japan), there were 17 consecutive patients with chronic hepatitis B who experienced >2 increases of >100 IU/L in ALT level and for whom stored serum samples were available. These 17 patients were enrolled in this study, among whom 33 such increases in ALT level were observed. Thirteen of 17 patients received IFN treatment, usually during an increase in ALT level. The clinical profiles of these 17 patients are shown in table 1. Written informed consent was obtained from all patients, and the study was approved by the Hiroshima University Ethics Committee.

HBV markers. Hepatitis B e antigen and antibody against e antigen were quantified by use of enzyme immunoassay kits (Abbott Diagnostics). HBV DNA was measured by use of real-time PCR performed with the 7300 Real-Time PCR System (Applied Biosystems), in accordance with the manufacturer's instructions. The primers used for amplification were 5'-TT-

TGGGCATGGACATTGAC-3' (nt 1893–1912; nucleotide numbers are those of HBV subtype C as reported by Norder et al. [30]) and 5'-GGTGAACAATGTTCCGGAGAC-3' (nt 2029–2049). For real-time PCR, we used 25 μL of SYBR Green PCR Master Mix (Applied Biosystems) with 1 μL of the DNA solution and 200 nmol/L of each primer. The amplification conditions were as follows: 2 min at 50°C, 10 min at 95°C, followed by 40 cycles of amplification (denaturation at 95°C for 15 s and annealing and extension at 60°C for 1 min). The lower detection limit of this assay was 10^3 copies/mL.

Extraction of HBV DNA and quantitative analysis of hypermutated genomes. HBV DNA was extracted from 100-μL serum samples by use of the SMITEST DNA Extraction Kit (Genome Science Laboratories) and dissolved in 20 μL of water. Hypermutated genomes were quantified by use of TaqMan 3D-PCR performed with the 7300 Real-Time PCR System (Applied Biosystems); we used a procedure described elsewhere [28], with slight modifications. In brief, the HBV DNA fragments were amplified by use of 3D-PCR in which the denaturation temperature was set lower than usual so that only G-to-A hypermutated genomes would be amplified. The amplification conditions were as follows: activation at 95°C for 10 min; followed by initial denaturation at 89°C for 20 min, to allow nonhypermutated genomes reanneal; and 45 cycles of amplification (denaturation at 89°C for 20 s, annealing at 50°C for 30 s, and extension at 62°C for 90 s). TaqMan PCR was performed using the following primers: 5'-ACTTCAACCCCAACAMRRATCA-3' (nt 2978–2999) and 5'-AGAGYTTGKTGGAATGTKGTGGA-3' (nt 24–1), where M is A or C, R is G or A, Y is T or C, and K is G or T. The probe was a 6-carboxyfluorescein (FAM)–labeled MGB probe, 5'-(FAM)-TTAGAGGTGGAGAGATGG-(MGB)-3' (nt 3184–3167). The detection limit of hypermutated genomes was 10^2 copies/mL, and nonhypermutated genomes were not amplified by 3D-PCR [28]. The reproducibility of the assay was quite high (as indicated by the small standard deviation relative to the results of the quantitative PCR control reaction), as reported in our previous study [28].

Cell culture and transfection. HepG2 cell lines were grown in Dulbecco's modified Eagle medium supplemented with 10% (vol/vol) fetal calf serum at 37°C in 5% CO_2. Cells were seeded to semiconfluence in 6-well tissue culture plates and transfected with the plasmid pTRE-HB-wt, which contained 1.4–genome length wild-type HBV genomes [31], by calcium phosphate precipitation. Seventy-two hours after transfection, the supernatant was collected for HBV DNA quantification by real-time PCR and for quantitative analysis of G-to-A hypermutated genomes [28]. The remaining supernatant was stored at −80°C for infection experiments using human hepatocyte–chimeric mice.

Quantitative analysis of G-to-A hypermutated genomes with human hepatocyte–chimeric mice. A human hepatocyte–chimeric mouse model was developed, as described previously [32], and used in infection and IFN-treatment experiments. The human hepatocytes progressively repopulated the murine host liver and were susceptible to HBV produced in cultured cell lines [31]. All animal protocols were in accordance with the guidelines of the local animal experimentation committee. The experimental protocol was approved by the Ethics Review Committee for Animal Experimentation of the Graduate School of Biomedical Sciences, Hiroshima University. Hepatocyte-chimeric mice were inoculated with 500 μL of the supernatant produced by transiently transfected cell lines. After confirmation of high-level HBV viremia, the mice were treated with 7000 IU/g/day of IFN-α, injected intramuscularly, for 14 days (the IFN-α was a gift from Hayashibara Biochemical Labs in Okayama, Japan). Human serum albumin in mouse serum was measured with the Human Albumin ELISA Quantitation Kit (Bethyl Laboratories), used in accordance with the manufacturer's instructions.

Statistical analysis. Differences between clinical groups with respect to HBV DNA and e antigen levels were examined for statistical significance, using the Mann-Whitney *U* test. A *P* value $<.05$ was considered to indicate a statistically significant difference. All statistical analyses were performed with StatView (version 5.0; SAS Institute).

RESULTS

Clinical course of disease in patients with increased ALT levels and fluctuations in the number of hypermutated genomes. Figure 1*A*–1*D* shows clinical courses for 4 representative patients (patients 1–4 in Table 1) with chronic HBV infection who experienced increases in ALT level. We observed marked decreases in HBV DNA level in association with marked increases in hypermutated genomes (figure 1*A*–1*C*, black arrows). In contrast, there was no apparent reduction in HBV level in the absence of an increase in hypermutated genomes (1*A*–1*D*, white arrows). We also analyzed the effect of IFN therapy on the number of hypermutated genomes. In some patients, we observed an increase in the number of hypermutated genomes during IFN therapy (figure 1*B* and 1*C*) as well as a marked increase in the number of hypermutated genomes and a reduction of the virus accompanied by an increase in ALT level just after cessation of IFN therapy (1*A*–1*C*, black arrows). However, in some patients, such as patient 1 (figure 1*A*), we observed no apparent increase in the number of hypermutated genomes in response to IFN therapy. However, the number of hypermutated genomes observed in samples from this patient obtained just before the initiation of IFN therapy (996/10^6 genomes) was already higher than the baseline level (157/10^6 genomes). Samples from patient 4 (figure 1*D*) showed an increase in the number of hypermutated genomes during IFN therapy (1907/10^6 genomes), though this is less than the increase observed during natural exacerbation (12,404/10^6 genomes). In fact, there was no significant difference between IFN-treated patients and untreated patients with respect to the number of hypermutated genomes observed (data not shown). These results suggest that the host's antiviral immunity level was higher at baseline than it was after

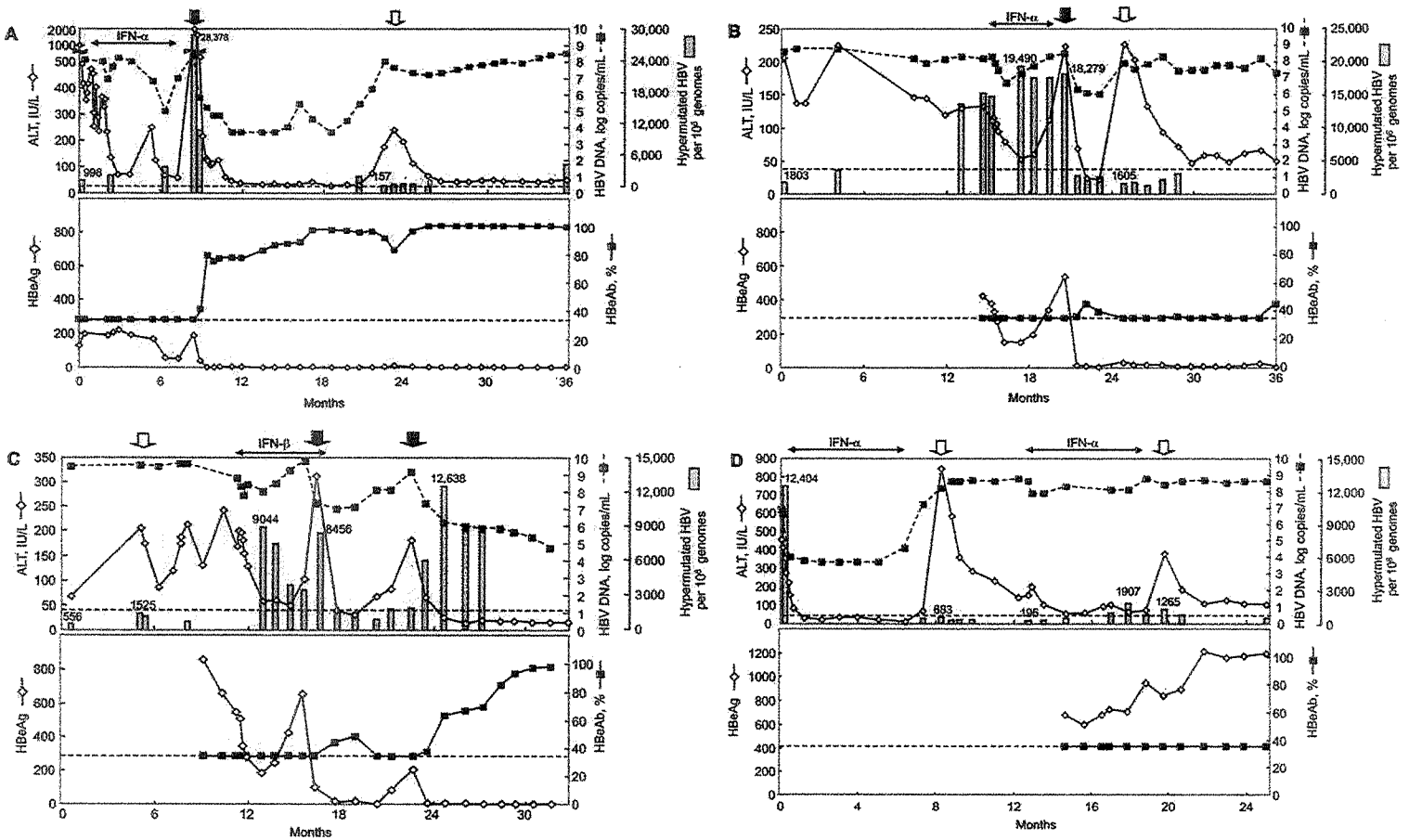

Figure 1. Clinical courses for 4 patients *(A–D)* with chronic hepatitis B virus (HBV) infection who experienced exacerbation of infection. *Black arrows,* exacerbation associated with an increase in the number of hypermutated genomes (>5 times basal levels); *white arrows,* exacerbation not associated with an increase in the number of hypermutated genomes; *horizontal dotted lines,* upper normal limit of alanine aminotransferase (ALT) (40 IU/mL; *upper panel, A–D*) and the detection limit for antibody against e antigen (HBeAb) (35%; *lower panel, A–D*). HBeAb, antibody against HBV e antigen; HBeAg, HBV e antigen; IFN, interferon.

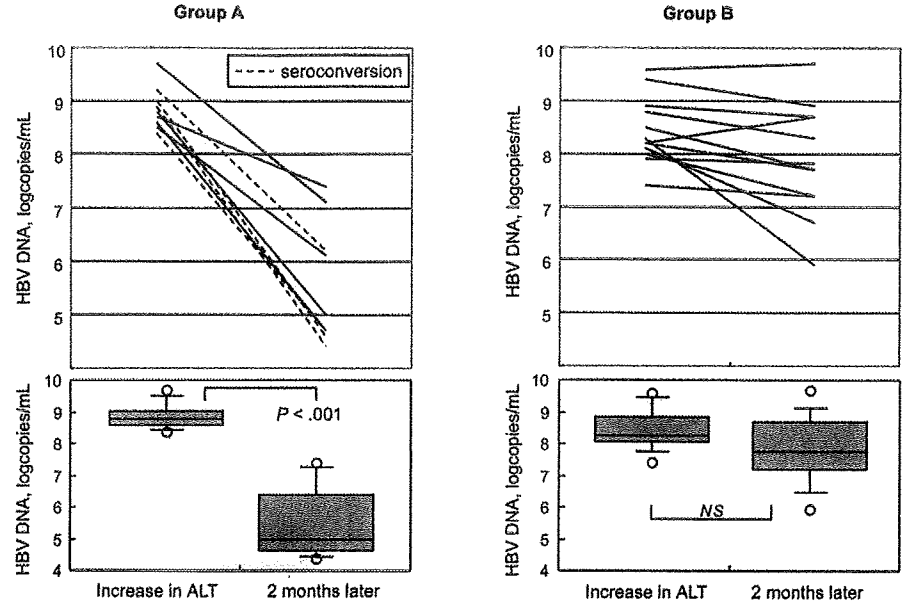

Figure 2. Relationship between increase in the number of hypermutated genomes and plasma levels of hepatitis B virus (HBV) DNA in 17 patients with chronic HBV infection who experienced >2 increases of >100 IU/L in alanine aminotransferase (ALT) level. Patients' exacerbations were divided into 2 groups, A and B, according to the extent of increase in the number of hypermutated genomes, relative to the basal number (group A included 9 exacerbations that involved a >5-fold increase in the number of hypermutated genomes; group B included 12 exacerbations that involved a ≤5-fold increase in the number of hypermutated genomes). *Upper panel* for groups A and B, individual HBV DNA levels at the time the ALT level increased and 2 months later; in the upper panel for group A, *dashed lines* indicate 4 exacerbations associated with seroconversion to positivity for antibody against e antigen. *Lower panel* for groups A and B, box-and-whisker plots for HBV DNA levels at same 2 time points. In the plots, the lines in the boxes indicate median values; the upper and lower lines of the boxes indicate the 25th and 75th percentiles, respectively; and the upper and lower whiskers represent the 90th and 10th percentiles, respectively.

IFN or that the feedback system for IFN signaling was already active before initiation of therapy.

We also compared the degree of reduction in the plasma HBV DNA level for exacerbations (i.e., increases in ALT level) associated with a marked increase in the number of hypermutated genomes (i.e., those in which the peak number was >5 times the number observed prior to exacerbation) and for exacerbations not associated with such an increase. As shown in figure 2, 8 of 9 exacerbations that were coupled with a marked increase in the number of hypermutated genomes (group A) were associated with a >2-log reduction in the HBV DNA level. In contrast, only 1 of the 12 exacerbations not associated with a marked increase in the number of hypermutated genomes (group B) was associated with a >2-log reduction in plasma HBV DNA level. The median serum HBV DNA level decreased from 8.8 to 5.0 log copies/mL among the patients in group A ($P < .001$) but did not decrease for patients in group B (figure 2).

In addition, we compared the reduction in e antigen level for these 2 groups. Levels were reduced in both groups, but the median reduction was more prominent for patients in group A than for those in group B (figure 3). All 4 exacerbations coupled with e antigen seroconversion (from positive to negative) were associated with marked increase in hypermutated genomes (figure 3).

Effect of IFN treatment on the rate of HBV hypermutation in chimeric mice. Next, we examined the effect of IFN treatment on G-to-A hypermutation in HBV genomes in human hepatocyte–chimeric mice. Two mice were intravenously injected with supernatant produced by HepG2 cells transiently transfected with a plasmid containing 1.4–genome length wild-type HBV genomes. Ten weeks later, after confirmation of high-level HBV viremia, the mice were treated with 7000 IU/g/day of IFN-α, injected intramuscularly, for 14 days. We observed an ~1.5-log reduction in plasma HBV DNA level accompanied by an increase in the number of hypermutated genomes in both mice (figure 4*A*). In a mouse inoculated with HBV but treated with phosphate-buffered saline, no increase of hypermutated genomes was observed (figure 4*B*). We also observed a 36-fold increase in the level of APOBEC3G mRNA, as determined by human oligonucleotide microarray (data not shown).

Infectivity of hypermutated genomes. To study the biological significance of hypermutated genomes, culture supernatant from HepG2 cells transfected with both HBV and APOBEC3G (5 μg each) was injected into a chimeric mouse. As shown in figure 5, the culture supernatant contained a large number of hypermutated genomes. In contrast, we could not detect hypermutated genomes in the chimeric mouse inoculated with this